# Mobile measurements for distribution and attribution of particulate matter in urban environments

Lorenz Harr [a,*], Tim Sinsel [a], Helge Simon [a], Max Carl Arne Torbenson [a], Esper Jan [a,b]

[a] Department of Geography, Johannes Gutenberg-University, Johann-Joachim-Becher-Weg 21, 55128, Mainz, Germany
[b] Global Change Research Institute of the Czech Academy of Sciences (CzechGlobe), 60300, Brno, Czech Republic

## HIGHLIGHTS

- $PM_1$ and $PM_{10}$ are significantly higher in the morning than in the afternoon.
- $PM_1$ and $PM_{10}$ are 13 and 31% higher in urban compared to surrounding rural areas.
- Particle numbers decrease significantly with increasing diameter along the track.
- Total mass is bi-modally distributed and dominated by particles <0.3 μm and 3–5 μm.
- Mass diameter distributions indicate traffic as main emission at urban hotspots.

## ARTICLE INFO

## ABSTRACT

Particulate matter (PM) sources differ in urban environments and may show spatiotemporal distinct patterns for varying particle aerodynamic diameters ($D_P$). We here assess such patterns using high-resolution PM ≤10 μm data recorded with a cargo bike along a 14 km route through urban, suburban, and rural areas in Mainz (Germany). The measurements conducted twice a day between May and August 2021 reveal decreasing particle number concentration (PNC) with increasing $D_P$ including ~6000 times higher particle numbers at $D_P$ 0.22–0.25 μm compared to $D_P$ 4–5 μm. Total mass concentration is bi-modally distributed and dominated by particles <0.3 μm and from 3 to 5 μm representing 36 and 22% of the entire air load, respectively. PM concentrations in Mainz are significantly higher in the morning than in the afternoon, and $PM_1$ and $PM_{10}$ are 13 and 31% higher in urban compared to surrounding suburban and rural areas. The high-resolution measurements also revealed 30% higher PM concentrations at $D_P$ 3–5 μm in the urban compared to the rural sectors, which is indicative for road dust, brake and tyre abrasion as the main source. $D_P$ distribution in rural hotspots is generally shifted toward larger particles >3 μm, most likely related to natural dust from agricultural fields. These findings show that high-resolution PM profiles can skillfully be recorded using bikes as mobile platform to identify spatial pollution patterns and attribute $D_P$ spectra to particular emission sources.

## 1. Introduction

Ambient air pollution is identified as one of the major health risks worldwide (WHO, 2022). Air pollutants such as PM cause cardiovascular and respiratory diseases, which can lead to premature deaths (Lelieveld et al., 2019). While $PM_{10}$ – particles with aerodynamic diameter ($D_P$) of <10 μm – is inhalable and reaches in to lungs, fine particles with $D_P$ <2.5 μm ($PM_{2.5}$) can get to the bronchial system and cause lung disfunction as well as chronic obstructive pulmonary disease (Gualtieri et al., 2011; Torres-Ramos et al., 2011). For these reasons,

both particle fractions are regulated by the EU with a permissible annual mean concentration of 20 and 40 μg/m$^3$ for $PM_{2.5}$ and $PM_{10}$, respectively, as well as with daily thresholds of 50 μg/m$^3$ for $PM_{10}$ which must not be exceeded more than 35 times a year (EU, 2008). Finer particles like $PM_1$ – particles with $D_P$ <1 μm – are not regulated, although high $PM_1$ exposure is even worse than $PM_{10}$ and $PM_{2.5}$: $PM_1$ can reach deeper into the lungs causing poorer lung functions, cytotoxicity effects and inflammation, particularly affecting children (Jalava et al., 2015; Yang et al., 2020).

In urban environments, the level of PM depends largely on regional

---

background concentrations and local emission sources, including mineral and biogenic components, but also of anthropogenic origins, i.e. domestic heating, industrial fumes and particularly traffic (e.g. Azarmi et al., 2016; Karagulian et al., 2015; Minguillón et al., 2012; Titos et al., 2014). Traffic-related emissions are not of homogenous particle sizes, since they are released by different processes: While combustion exhausts of motorized vehicles mainly emit particles with $D_P < 1$ µm (Squizzato et al., 2016; Titos et al., 2014), non-exhaust particles – i.e. road wear, (resuspended) road dust as well as tyre and brake abrasion – contribute to mass concentration of particles with $D_P$ 1–10 µm (Harrison et al., 2021; Piscitello et al., 2021) with $D_P$ of tyre and brake abrasion mainly ranging between 2–5 µm and 1–6 µm, respectively (Fussell et al., 2022; Hussein et al., 2008; Oroumiyeh and Zhu, 2021).

An identification of emission sources by particle size is therefore only possible if the particles were measured in (sub-) micron resolution. Official stationary monitoring networks in Europe, however, were not able to resolve particle sizes in this range as they were providing only $PM_{10}$, $PM_{2.5}$ and (rarely) $PM_1$ data according to the legal requirements (European Parliament and Council, 2008). In addition, the immobility of the stations and their temporal measurement resolution of >30 min averages (ZIMEN, 2022) make it unfeasible to record variations in urban PM concentrations, for example induced by changes in traffic intensity or varying street characteristics, e.g. between street canyons and open building arrangements (Bukowiecki et al., 2010; Gallagher et al., 2015).

These spatiotemporal gaps can be closed by mobile measurements that allow high spatial coverage to be extended both horizontally and vertically, for example to breathing height level of pedestrians to assess personal exposure, but also to identify hotspots (Elen et al., 2012). Mobile PM measurements were mainly conducted on foot or by bicycle as they do not include emission source that might interfere with the measurements (e.g. Carreras et al., 2020; Garcia-Algar et al., 2015; Harr et al., 2022b; Sharma and Kumar, 2020). While studies by foot only allow high spatiotemporal measurements in short time intervals (>1s) along a max. 5 km long track within an hour (Harr et al., 2022a), measurements by bicycle enable covering a larger area at the same time span, e.g. areas of different characteristics like urban, suburban, and rural within the same run. However, there is only a limited number of studies that conducted mobile PM measurements using bicycles: Most studies focused on PNC of ultrafine particles (UFP) or particles <10 µm, as well as of $PM_1$, $PM_{2.5}$ and $PM_{10}$. Berghmans et al. (2009), for example, used their bicycle platform Aeroflex II to investigate the exposure of cyclists to UFP and $PM_{10}$ in the town of Mol, Belgium. They found out that UFP concentrations were highly variable within the same microenvironment due to changes in traffic and building activities as main emission sources. Boogaard et al. (2009) confirmed these results in their mobile bicycle measurements in 11 midsized Dutch cities finding that UFP concentrations were highly variable and, additionally, their peaks were not correlated to $PM_{2.5}$ hotspots. Carreras et al. (2020) and Klemm et al. (2021) investigated in their studies with a cargo bike platform in the city of Aachen, Germany, that the choice of route could be a key factor to reduce cyclist exposure to particulate matter <10 µm as traffic emission sources had the most impact on particulate matter. Van den Bossche et al. (2015) as well as Samad and Vogt (2020) additionally measured nitrogen oxides, ozone and black carbon by bicycle in the city center of Antwerp, Belgium and Stuttgart, Germany, respectively, to map spatial variability in urban environments. To address emission sources, however, these approaches can be imprecise because the used PM and PNC fractions might not resolve the particle distributions sufficiently.

The novelty of our approach is to quantify the spatiotemporal variability and distribution of PM and PNC in high, (sub-) micron resolution of 31 different $D_P$ to determine its emission sources in different urban environments in the morning (MO) and afternoon (AF). In this study, we (i) compare measured $PM_1$ and $PM_{10}$ of approx. 50 MO and AF runs with stationary data, (ii) analyze their spatial variability to identify hotspots, (iii) quantify the measured PNC and mass concentrations per $D_P$, and

(iv) discuss the relative differences per $D_P$ to identify emission sources at the hotspots.

## 2. Material and methods

### 2.1. Study site

The measurements were conducted from 28th May to August 5, 2021 in Mainz, the capital and largest city (approx. 220,000 inhabitants) of the southwestern German federal state Rhineland-Palatinate (50.0° N, 8.26° E, Fig. 1). Mainz is an inland town located in a gently hilly landscape along the River Rhine, which features a moderate climate with an annual average temperature of 10.7 °C and precipitation of 620 mm (Koeppen Cfb; DWD, 2021a; 2021b). The city's basin location hinders large-scale air exchange and results in Mainz being one of the most polluted cities in Germany (ZIMEN, 2021). The 14 km long, circular study route led on paved roads through areas of different characteristics: While the starting and ending point at the campus of the university (49.9932° N, 8.242° E; Fig. 1 (1)) was characterized by large low-rise buildings and low traffic, the route passed down the hill streets with predominantly compact midrise buildings and multi-lane roads of high traffic intensity in the city center (Fig. 1 (2,3)). The route exited downtown via the steep and narrow, three-stories high street canyon 'Gaustraβe' (<10 m wide, building-height-to-width ratio ~1) (Fig. 1 (4)) onto the high traffic multi-lane road 'Pariser Straβe' leading out of town (Stewart and Oke (2012); Fig. 1 (6)). At the town sign, the route continued through a suburban area with low-rise buildings and low traffic followed by an agricultural area in the west of the city (Fig. 1 (7)), before returning to the starting/ending point at the campus. We conducted two measurement runs every day starting at 7:30 a.m. and 4:30 p.m. to cover MO and afternoon AF rush hour times.

The mobile measurements were conducted with a full-suspension electro cargo bike. The electric assistance allowed measurements to be made at a constant, average speed of 17 km/h and the suspension avoided vibrations which could interfere with the measurements. The bike was equipped with a GPS device powered by an USB-Powerbank and a camera with which each run was filmed to facilitate the identification of local emitters during the post analysis process (Fig. 2). As PM sensor, a GRIMM 11-R laser aerosol spectrometer was mounted in a box on the cargo platform, with the front orientated air inlet at a height of 1.6 m, corresponding to the average breathing height of adults. The GRIMM 11-R is an optical particle counter following the light scatter principle (Mie, 1908) and is able to count particle sizes from 0.25 µm to 32 µm with 31 size bins in high temporal resolution of 6 s (GRIMM Aerosol Technik GmbH & Co. KG, 2015). The instrument is calibrated by the manufacturer to a filter-based reference instrument (Peters et al., 2006). As the GRIMM 11-R is intended for indoor use, it should only be used at RH <95% and under precipitation-free conditions, as condensation could significantly damage the unit's optical chamber.

### 2.2. Postprocessing analysis

Several postprocessing steps had to be conducted to enable a reliable spatial analysis of each run's measurement. At first, the GRIMM measurements were merged with the GPS data. To avoid slight spatial inaccuracies and minor variations between the runs, a spatial synchronization to a manually set ideal route was applied. An ideal route was converted into datapoints with a distance of 10 m and assigned the 10 closest original measurement points to each point using inverse distance weighting (Shepard, 1968). The PM data were subsequently linearly detrended to mitigate potential time-related changes in particle concentrations along the study route (Harr et al., 2022a). The differences between MO and AF concentrations in $PM_1$ and $PM_{10}$ were tested on significance using a Monte Carlo simulation approach in which for 1000 iterations 100 AF and MO datapoints were randomly taken to calculate paired Mann-Whitney U tests. We then calculated the quartile

**Fig. 1.** Bicycle track in Mainz (black line) with photographs from the starting and ending point at the university **(1)**, the Kaiserstraße **(2)**, Rheinallee **(3)**, Gaustraße **(4)**, Fichteplatz **(5)**, Pariser Straße **(6)** and agricultural area **(7)**. The monitoring sites at Mainz-Zitadelle and Friedrichsfeld are highlighted by black dots. Insert map shows the location of Mainz (orange) in Germany. © OpenStreetMap.



**Fig. 2.** Photographs of the electro cargo bike with GPS device, powerbank, camera **(a)** and the box containing PM sensors, GRIMM 11-R PM sensors **(b)**.

coefficient of dispersion (QCD) to quantify the variation of particle concentrations along the study route, since this measure of variation is less sensitive to outliers than the commonly used coefficient of variation (Bonett, 2006).

To specify the particle distribution of the particle number (PNC) and mass concentrations (dM) of the mean MO and AF runs, the standard PM categories of $PM_1$, $PM_{2.5}$, and $PM_{10}$ were considered too imprecise. We hence focused on the originally measured PNC and dM instead, which is divided into 31 $D_P$ bins ranging from <0.25 μm to 32 μm (GRIMM Aerosol Technik GmbH & Co. KG, 2015). These datasets were then used to calculate median PNC and dM for each particle $D_P$ category at each datapoint along the study route for the average of all MO and AF runs, respectively. A normalization of the dM data was performed with $dM/dlog(D_P)$ to reduce possible bias in the $D_P$ masses due to unequal bin widths at each point on the track. Finally, relative differences between dM and $dM_{MEDIAN}$ of each $D_P$ were calculated to indicate the relative

particle distribution for each particle bin size along the study route.

## 3. Results and discussion

### 3.1. Mean $PM_1$ and $PM_{10}$

During the study period, 97 of 140 possible measurement runs (50 MO and 47 AF runs) could be conducted, 43 measurement runs were omitted due to unstable weather (Fig. S1). These unsteady weather conditions – precipitation was 27% higher than in the reference period 1991–2020 (DWD, 2022) – led to cleaner air with relatively low particle concentrations overall: There was no run in which mean $PM_{10}$ exceeded the daily threshold of 50 μg/m$^3$ stated in the European law (European Parliament and Council (EU), 2008). Nonetheless, the spatially averaged mean $PM_1$ and $PM_{10}$ concentrations recorded with the cargo bike were in line with the mean of 3-min averaged values at the stationary monitoring station Mainz-Zitadelle at the same time in MO and AF, provided by a Thermo Fisher Sharp 5030 measurement instrument of the ZIMEN network (ZIMEN, 2022) (Fig. 3). The absolute differences between mobile and stationary measurements, however, were higher in $PM_{10}$ (mean$_{DIFF\_PM10}$ = 2.1 μg/m$^3$; sd$_{DIFF\_PM10}$ = 7.4 μg/m$^3$) than in $PM_1$ (mean$_{DIFF\_PM1}$ = 0.6 μg/m$^3$; sd$_{DIFF\_PM1}$ = 1.5 μg/m$^3$), whereas the measured mean values were in at least 68% of the runs for $PM_1$ (73% for $PM_{10}$) higher than the stationary data. The higher concentrations might be caused by the different inlet heights of the PM sensors. While PM was measured on 3.6 m at the monitoring station, the inlet of PM sensor on the cargo bike platform is at 1.6 m, much closer to local emission sources near ground, i.e. traffic emissions. The variation of the $PM_{10}$ concentration levels could be caused by coarse particles emitted in the various local environments along the study route, e.g. road dust in the city vs. resuspended natural dust at the agricultural field (Kerschbaumer and Lutz, 2008). The comparison of mobile and stationary measurements underlines the feasibility of collecting reliable PM data with our mobile measurement setup by bike using GRIMM 11-R in urban environments.

### 3.2. Spatial pattern of $PM_1$ and $PM_{10}$

The spatial pattern of mean $PM_1$ and $PM_{10}$ along the study track showed higher concentrations in the city than in the suburban and agricultural area (Fig. 4a). However, these differences were rather small for $PM_1$, as absolute differences were only 1.5 μg/m$^3$ (13%) between 'Rheinallee' (Fig. 1 (4)) – a high traffic location with the highest mean values – and the traffic-calmed university campus (Fig. 1 (1)). For $PM_{10}$, the difference between the highest concentrations, 'Gaustraβe' (Fig. 1 (4)), and the lowest, also university campus, was 6.3 μg/m$^3$, meaning a

relative difference of 31%. It is evident that the concentrations of both $PM_1$ and $PM_{10}$ were significantly higher in the MO than in the AF, regardless of the location along the route (Fig. 4 b). The mean differences between MO and AF were 3.7 μg/m$^3$ (~54%) for $PM_1$ and 7.7 μg/m$^3$ (~62%) for $PM_{10}$, whereas the $PM_1/PM_{10}$ ratio rose from 53% to 58% on average. The relative differences of $PM_1$ and $PM_{10}$ during the day were very similar and could be explained by the average atmospheric conditions. During the night, high convective inhibition values and low windspeeds indicate low, stable mixing layers leading to higher suspension of particles near ground. During the day, solar forcing in combination with diurnal temperature differences of >10 K led to fast dissolving of the stable mixing layer by thermal convection which in turn caused lower PM concentrations for the AF runs (Tang et al., 2016; Wagner and Schäfer, 2017); Fig. S1).

Nonetheless, the variation of $PM_1$ was only 12%, resulting in small differences in concentrations along the route with no clear local hotspot in the mean MO and AF runs. In contrast, the variation of $PM_{10}$ is larger along the study track, whereby the QCD is higher in AF than in MO (0.38–0.31). Moreover, three local $PM_{10}$ hotspots could be additionally identified for both times of the day, the 'Kaiserstraβe', the 'Gaustraβe' and the 'Pariser Straβe' (Fig. 1 (2,4,6)) and another one close to a farm house in the agricultural fields (10.4 km) in AF. These hotspots become even more visible during mean MO runs, where $PM_{10}$ showed differences of >2 μg/m$^3$ between hotspot and surrounding streets, with a maximum value of 5.7 μg/m$^3$ at the 'Gaustraβe'.

### 3.3. Particle numbers per $D_P$

The differences in variation between $PM_1$ and $PM_{10}$ indicate that $PM_{10}$ hotspots were mainly caused by particles larger than $PM_1$. However, the PNC per originally measured $D_P$ bin of the sensor showed that, regardless of the time of the day and the position on the measurement track, most particles were assigned to the smallest $D_P$ (Fig. 5). PNC decreased sharply with increasing $D_P$. PNC with $D_P$ < 0.25 μm, for instance, reached up to ~600,000 counts per liter, whereas PNC for the largest bin with continuously measured PM, $D_P$ of 4–5 μm, was around 100 particles per liter. Consequently, particles with $D_P$ of <1 μm account for <58% of the $PM_{10}$. PNC with $D_P$ of <0.25 μm is even more than 2000 times higher than PNC with $D_P$ of 3.5–4 μm and even 6000 times higher than PNC with $D_P$ of 4–5 μm. The consideration of particle mass is hence probably not sufficient to describe the health hazards of especially small particles in a meaningful way (Schraufnagel, 2020).

An average of 191,501,376 particles (MO) was counted in comparison to a mean of 112,013,837 particles (AF), meaning that PNC was 71% higher in MO than in AF. This difference was even 9% higher than
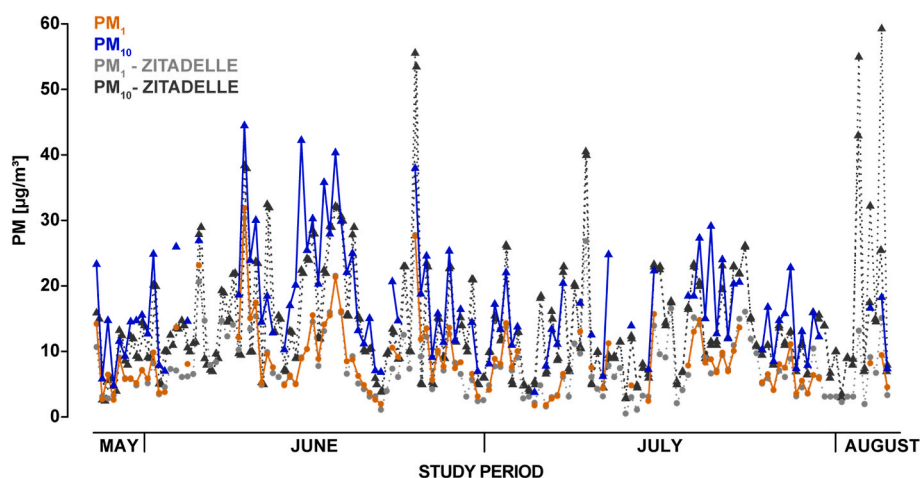


**Fig. 3.** Mean $PM_1$ and $PM_{10}$ concentrations from May–August 2021 recorded with the cargo bike and derived mean $PM_1$ and $PM_{10}$ from the official ZIMEN measurement station at Mainz-Zitadelle, respectively.
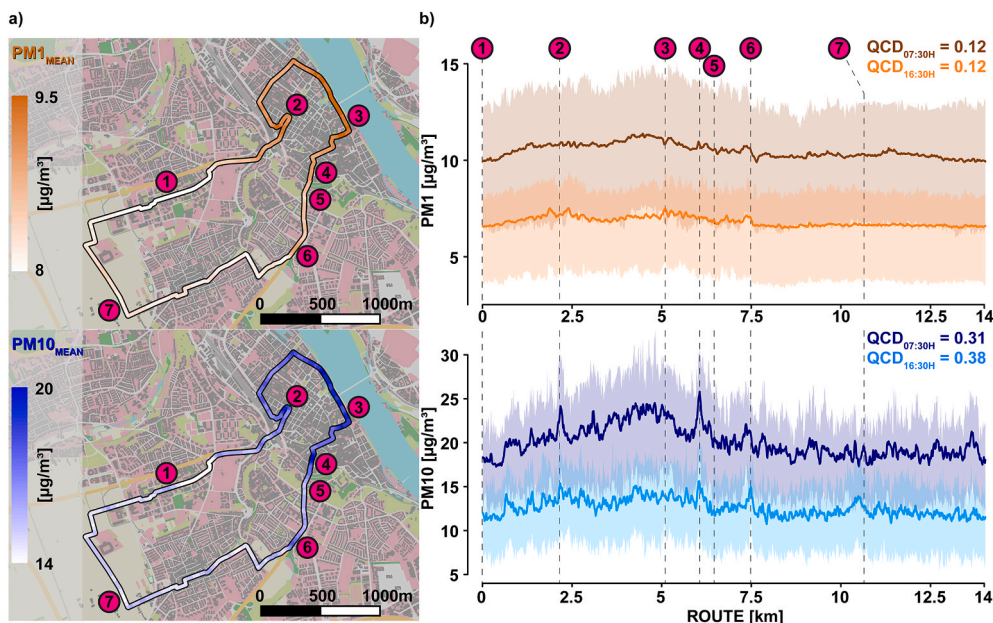
**Fig. 4.** Spatial patterns of mean PM$_1$ (brown) and PM$_{10}$ (blue) concentrations along the study track (a), and (b) subdivided into smoothed mean MO and AF timeseries (df = 35, n = 1403; dark and light colors, respectively) surrounded by the interquartile range in shaded colors.
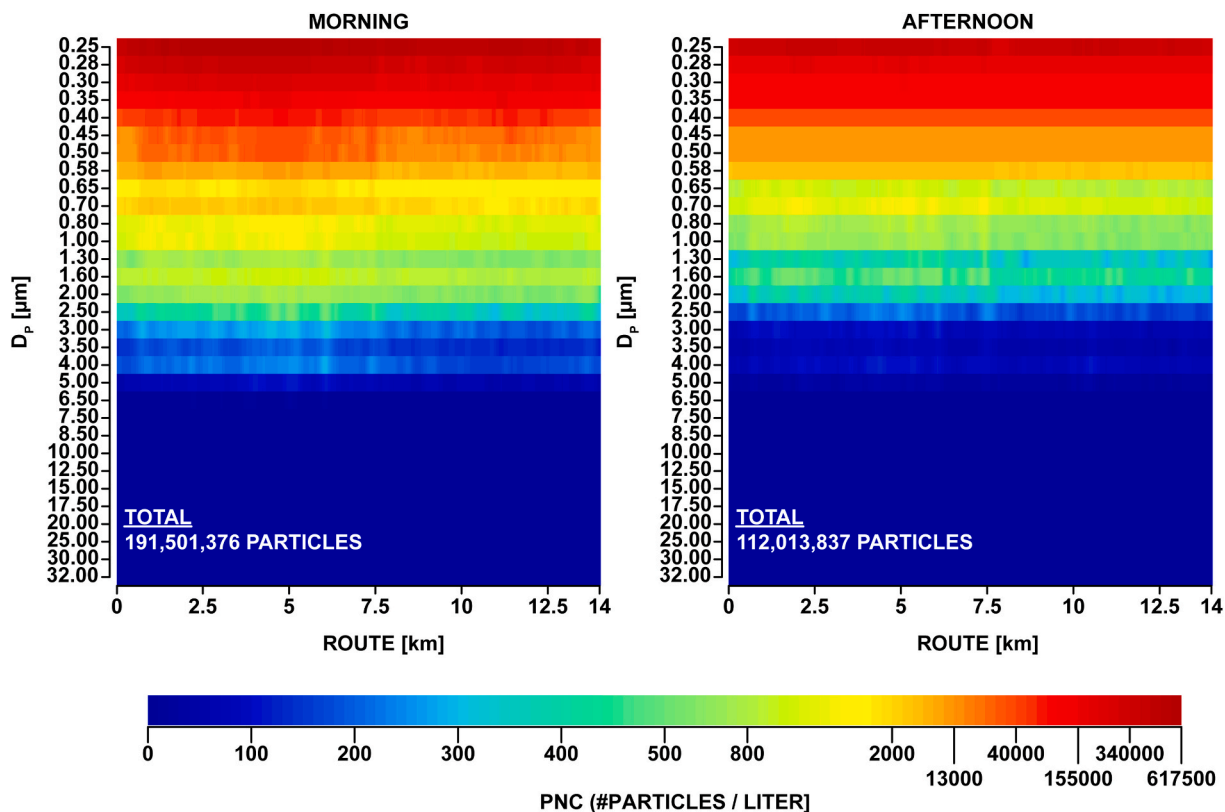


**Fig. 5.** Median PNC distributions for each bin along the study route in MO (left) and AF (right panel). Labels of the y-axes show the upper limit of the D$_P$ per bin.

between the PM$_{10}$ concentrations of the MO and AF runs, which could not be explained by additional particles with D$_P$ > 10 μm. It is more likely caused by uncertainties in the weighting process of the counted particle D$_P$ before calculating their dM (Morawska et al., 1999).

### 3.4. Median mass concentrations per D$_P$

The distribution of particle sizes along measured dM differed greatly from the distribution of particle counts showing that particles at D$_P$ of 0.22–0.25 μm and 3.5–5 μm were dominating the total dM, independently of the time of the day as well as the position on the route (Fig. 6a, left panel). In the averaged AF run, the dM for particles of 3.5–4 μm size

### a) MEDIAN MASS CONCENTRATION
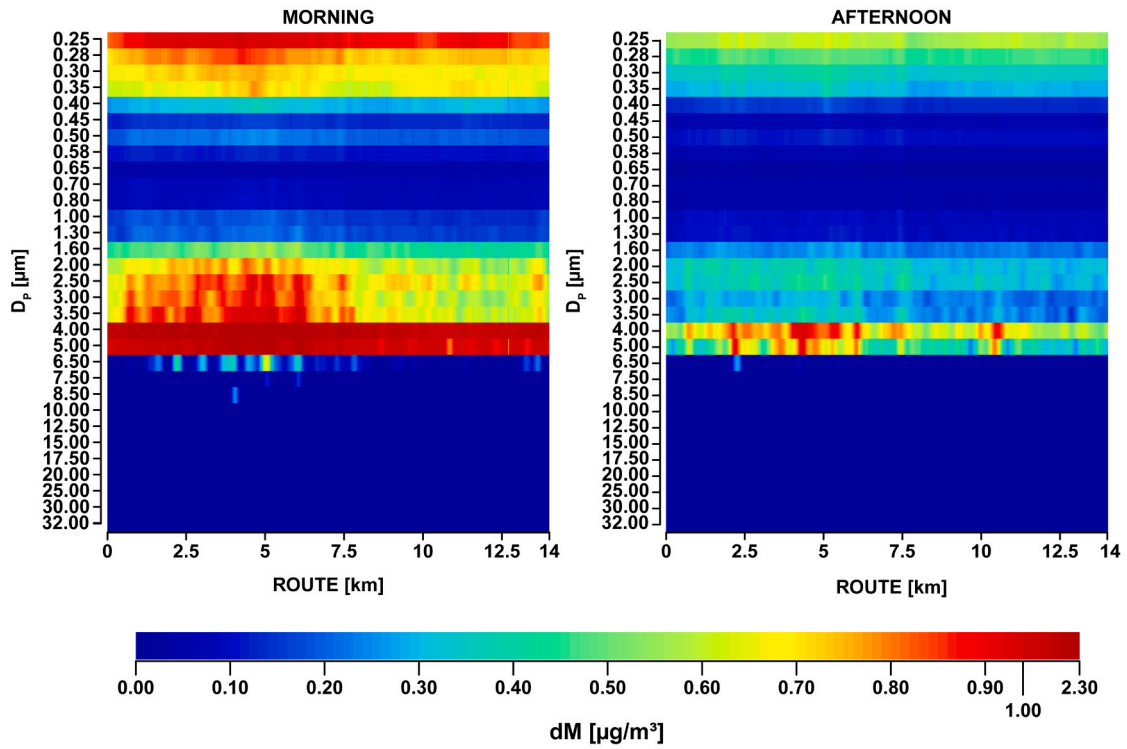


### b) NORMALIZED MEDIAN MASS CONCENTRATION
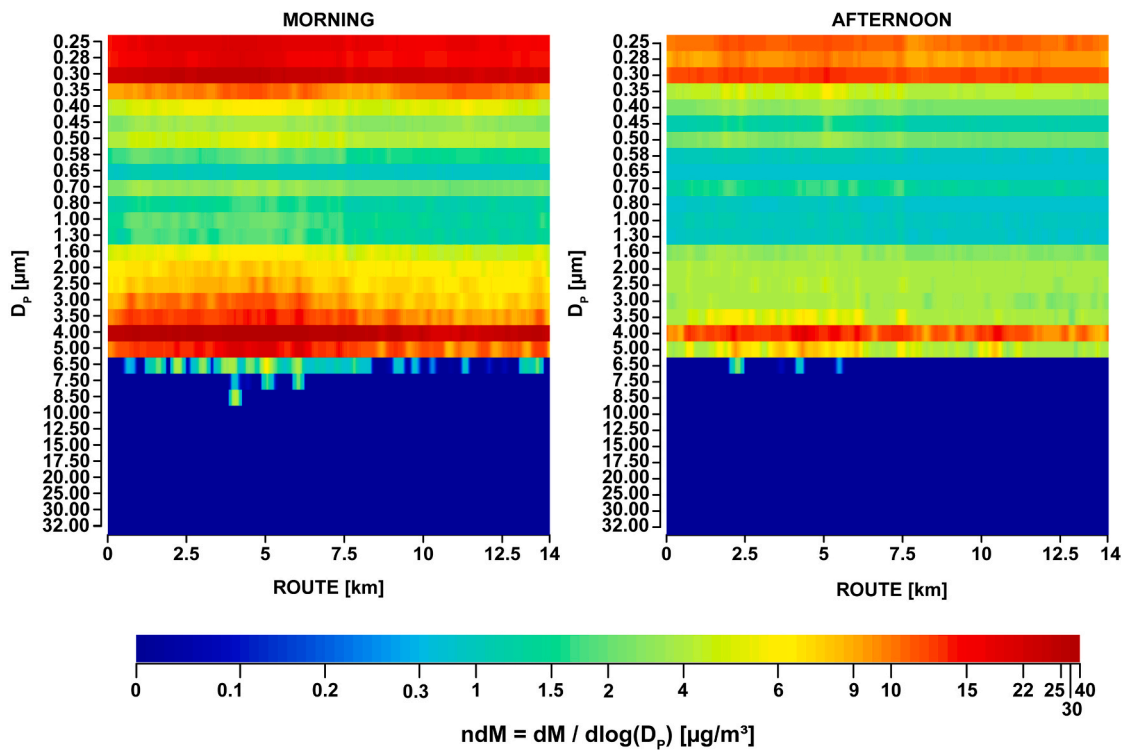


**Fig. 6.** Distribution of **(a)** median mass concentration (dM) and **(b)** normalized median mass concentration (ndM) per $D_P$ along the study route in the MO (left) and AF (right panel). Labels of the y-axes show the upper limit of the $D_P$ per bin.

ranged between 0.5 and 0.6 μg/m³ and 0.5–1 μg/m³, respectively, with hotspots in urban (max. 1 μg/m³; ~4.5 km) and agricultural (max. 0.9 μg/m³; ~11 km) areas. The averaged MO run showed higher dM values with 0.8–1 μg/m³ for the smallest $D_P$ and 1.2–2.3 μg/m³ for $D_P$ 3.5–4 μm, with highest values in the street canyon 'Gaustraβe' (Fig. 1 (3)). In contrast, particles with sizes of 0.35–1.3 μm contributed only by a maximum of 0.4 μg/m³ per $D_P$ (MO) and only by 0.2 μg/m³ per $D_P$ (AF) to the total dM of the runs – particles with $D_P$ 0.65 μm only by 0.05 μg/m³ for both times of the day. Moreover, the measured median dM shows a skewed picture of the particle mass distribution since the $D_P$ bins were not of equal width. This could cause an overestimation of the dM of large $D_P$, because the larger the $D_P$, the wider the bins and the higher the possibility of more particles in each bin. To reduce the biases, we calculated the 'normalized dM' (ndM) for every $D_P$ (Fig. 6b).

Particles with $D_P$ <0.3 μm showed still high ndM with >15.5 μg/m³ (MO) on average per $D_P$ and >9.5 μg/m³ (AF), whereas particles with $D_P$ of 0.28–0.3 μm had higher values than particles of $D_P$ 0.22–0.25 μm with 23.2 to 16.3 μg/m³ (MO) and 12.1 to 10.5 μg/m³ (AF). The small particle bins of $D_P$ < 0.3 μm contributed with >9% per $D_P$ to the total ndM and were only exceeded by particles with $D_P$ 3.5–4 μm having 27.6 μg/m³ and 12.0 μg/m³ on average, hence accounting with 16.3% and 14.4% (Fig. S2). Although particles with sizes between 0.35 and 1.3 μm accounted for maximum ndM values of 5.2 μg/m³ (MO) and 2.6 μg/m³ (AF) per $D_P$ on average, respectively, they contributed only by 3% per $D_P$ at both times of the day and thus did not have a major impact on the total ndM.

The distinct bimodal distributions in dM and ndM with peaks at DP 0.28–0.3 μm and $D_P$ 3.5–4 μm indicate different kinds of emissions: Particles with size of $D_P$ <0.3 μm originate from whirled-up road and mineral dust, and – in urban areas – from combustion-related processes, i.e. traffic exhausts (Karagulian et al., 2015; Squizzato et al., 2016). The peak in $D_P$ 3.5–4 μm point to (resuspended) road and mineral dust as particle sources, whereas mineral dust could be an integral part of the background concentration (Hussein et al., 2008; Titos et al., 2014).

According to Oroumiyeh and Zhu (2021), the main source of urban road dust could be locally emitted brake and tyre abrasion, as they have found out that brake and tyre wear have unimodal mass size distributions with a mode diameter of 3–4 μm and 4–5 μm, respectively. Studies by Sanders et al. (2003) and Lough et al. (2005) support the findings about the main size distribution of brake-related particles.

### 3.5. Relative differences per $D_P$

In order to indicate the spatial origin of the measured particles more clearly, we analyzed the relative differences of dM per $D_P$ along the route (Fig. 7). The relative differences between dM and $dM_{MEDIAN}$ per $D_P$ showed distinct higher values in the urban (1–7.5 km) than in the sub-urban and agricultural areas for all continuously measured $D_P$. For $D_P$ <1 μm, the concentrations were on average 13% (MO) and 14% higher (AF). The higher dM in the city could be attributed to locally emitted, traffic-related combustion processes and whirled-up road wear in the inner city which were largely absent in the suburban and agricultural areas. This hypothesis is in line with findings by Titos et al. (2014) showing that 16% of the total PM₁ concentrations at an urban station in southern Spain in summer were related to road dust and traffic exhaust, while the background concentration consisted of mineral dust (21%) and mainly of regionally transported, resuspended dust (63%). It is noticeable that the relative differences in the urban area were increasing with increasing $D_P$. While for $D_P$ 0.22–0.25 μm, the concentrations were 8% (MO) and 5% (AF) higher in the urban than rural areas on average, the difference of particles with $D_P$ 3–5 μm, mode diameter of tyre and brake abrasion, increased to 30%, at the 'Rheinallee' (3.7–5.1 km; Fig. 1 (3)) for particles with $D_P$ 4–5 μm even to 55% (MO) and 70% (AF). This discrepancy between dM in the city and dM in the more rural areas indicated a decreasing large-scale mixing with increasing size of the emitted particles. This behavior can be traced back to a shorter
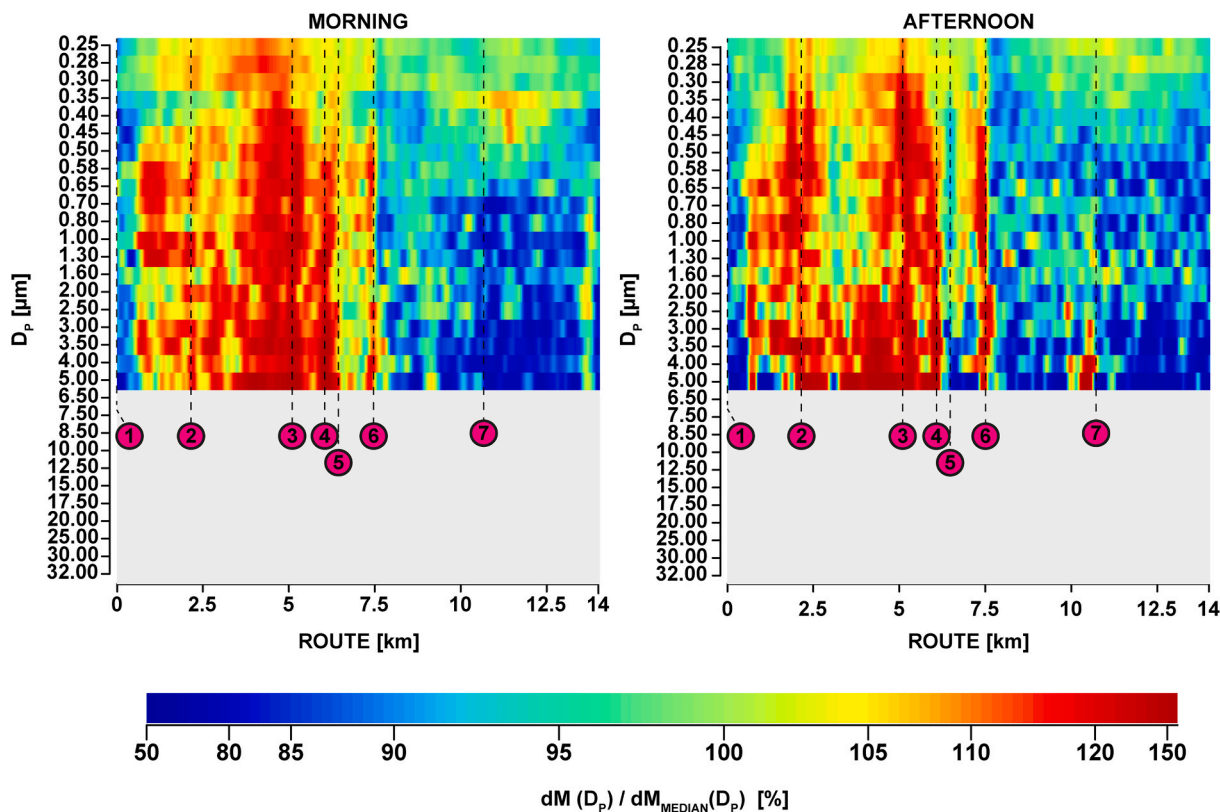


**Fig. 7.** Relative differences between dM and $dM_{MEDIAN}$ for each continuously measured aerodynamic diameter bin along the study route in the MO (left) and AF (right panel). Labels of the y-axes show the upper limit of the $D_P$ per bin. Dots and dashed lines refer to locations highlighted in Fig. 1.

suspension time of coarser particles in the ambient air due to faster deposition. Wu et al. (2018) found out that the velocity of dry deposition in summer for $PM_{10}$ (3.19 ± 1.18 cm/s) was nearly ten times higher compared to $PM_{2.5}$ (0.32 ± 0.33 cm/s) on average (i.e., the larger the measured particles, the more likely they have been emitted in the vicinity of the respective measurement). Our findings also agree with the results of Carreras et al. (2020), who stated in their study with mobile measurements of particle mass and number concentrations by bike, that long-range transported particles dominated the dM for $PM_{2.5}$, but local emissions were an important factor for coarse PNC concentrations with larger $D_P$. For the hotspot at the agricultural field (10.4 km) in AF runs, the relative differences for $D_P$ >3 μm were elevated by 20% compared to the $dM_{MEDIAN}$, indicating local emissions. In lack of motorized road traffic and as there were no other increased differences in smaller $D_P$, it is likely that the particles originated from locally whirled up natural dust from the surrounding fields. Considering the other identified hotspots at 'Kaiserstraße', 'Rheinallee', 'Gaustraße' and 'Pariser Straße' (see 3.2; Fig. 7 (2)–(4), (6)), the >17% higher relative differences of particles with $D_P$ >3 μm indicated that these particles have likely been locally emitted. Since concentrations were elevated across most diameters at these sites, it stands to reason that the particles were emitted from multiple sources at the same time or, more likely, from one source that emits particles with several $D_P$. In urban areas, this one source is traffic: Road wear and combustion processes of vehicles have an impact on particle concentrations of $D_P$ <1 μm (Titos et al., 2014), while (resuspended) road dust can also contribute to concentrations of particles with $D_P$ >1 μm (Fussell et al., 2022), predominantly at $D_P$ 3–5 μm due to brake and tyre abrasion (Hussein et al., 2008; Oroumiyeh and Zhu, 2021).

The patterns of the relative differences surrounding the hotspots support this hypothesis: While the relative differences were high on the entire, highly frequented, four-lane roads 'Kaiserstraße' (1.7–2.3 km) and 'Rheinallee' (3.7–5.1 km), the relative differences decreased greatly after the 'Gaustraße' and the 'Pariser Straße', which could be explained by the characteristics of the respective locations. At 'Pariser Straße' hotspot, the speed limit on the four-lane road is changed from 50 to 70 km/h for out-of-town traffic lanes, which leads to an acceleration of vehicles causing an increase in traffic exhaust and whirled up road dust on the one hand as well as increased braking on the opposite lanes on the other hand. This resulted in a rise in particle concentrations in each $D_P$, especially in $D_P$ >3 μm with relative differences of 113% (MO) and 124% (AF) on average. The differences at each $D_P$ decreased abruptly >20% as the bike lane leads away from the street into a suburban part of the town. The characteristics of the 'Gaustraße', however, are different. The 'Gaustraße' (5.9–6.4 km) is a short but steeply ascending road that is demanding for vehicles, leading to a higher amount of exhaust and brake abrasion particles. These particles accumulated due to the additional canyon effect in the street, as the surrounding buildings obstruct the air flow to disperse PM (Gallagher et al., 2015). This in turn resulted in up to 51% higher concentrations (MO) and even 61% (AF) for $D_P$ 4–5 μm in 'Gaustraße'. The relative differences for particles of the same $D_P$ decreased rapidly by 46% (MO) and 72% (AF) on average after leaving the street canyon and entering the 'Fichteplatz' (Fig. 1 (5)), an open place with scrubs and trees between the traffic and bike lane that reduces the impact of motorized traffic on the measurements. The more pronounced differences in AF occurred not only at 'Gaustraße' and 'Pariser Straße', but also at the other urban hotspots, which could be attributed to the generally lower concentration level with a higher diffusivity due to more solar forcing in AF (Tang et al., 2016; Wagner and Schäfer, 2017).

The dominance of traffic-related particle sources as local emissions in urban environments are not unexpected, but only the spatiotemporal high-resolution analysis of PM gave the possibility to attribute emissions from different processes to the same emission source, mainly tyre and brake abrasion and fuel combustion from traffic. This analysis can be particularly relevant since electric vehicles become a serious alternative

to internal combustion engine vehicles in urban environments (e.g. Ding et al., 2017; Sanguesa et al., 2021; Yong et al., 2015). Assuming an increasing proportion of electric vehicles, emission from combustion-related particles with $D_P$ <1 μm would be reduced to a minimum, which could lead to a reduction of up to 14% for total PM concentrations in urban areas. However, particle emissions by tyre and brake abrasion would still be present (Timmers and Achten, 2016; Woo et al., 2022), which means that the 30% higher particle concentrations in urban compared to rural areas at $D_P$ 3–5 μm will not decrease by banning fossil-fueled vehicles alone. In order to additionally minimize these PM concentrations, it would hence be required to reduce the total number of vehicles in the city, i.e., reducing private transport and increasing the use of local public transport.

Nonetheless, it is important to note that measurements of PNC and dM of particles alone could not prove the emission source beyond doubt, even though traffic is very likely one of the main PM sources in the city. It is also not possible to clearly distinguish between road dust and tyre and brake abrasion of the same size (Bukowiecki et al., 2010). We therefore recommend measuring the chemical composition of the particles in addition to the PNC and dM in further studies.

## 4. Conclusion

In this study, it was demonstrated that high-resolution spatiotemporal analyzes of particle numbers and particle mass concentrations in urban environments are feasible using a mobile measurement setup and produce values comparable to the fixed-station ZIMEN network. Mean $PM_1$ and $PM_{10}$ concentrations were higher in the urban than in the suburban and agricultural areas. Regardless of the unsteady weather conditions during the study period, PM concentrations were significantly higher in MO than in AF for both particle sizes. Whereas the $PM_1$ variability is somewhat reduced and shows no clear local hotspot, $PM_{10}$ variability is larger and can be used to identify pollution hotspot, three of which located at urban multi-lane roads and street canyons and one in the agricultural area. The numbers of particles per classified $D_P$ bin, however, showed that the PNC decreased greatly with increasing $D_P$. This finding is independent of the location and time of the day, and particle numbers were ~6000 times higher at 0.22–0.25 μm compared to 4–5 μm. Particles with $D_P$ <0.3 μm and 3–5 μm were vastly dominating, representing 33 and 24%, of the total dM, respectively. Higher dM in both of these $D_P$ ranges indicate that the particles were likely emitted from traffic-related combustion processes ($D_P$ < 1 μm) and tyre and brake abrasion ($D_P$ 3–5 μm). In contrast, the AF hotspot in the agricultural area showed a relative increase of 20% at $D_P$ >3 μm indicating natural dust from the fields as the main source. These might be relevant for traffic planning as the transition from fossil-fueled to electric vehicles in urban areas can reduce the PNC for DP <1 μm significantly and the dM would decrease up to 14%. However, tyre and brake emissions would still be present and harmful particularly in street canyons and roads with high traffic intensity. A reduction of the total number of vehicles and increase of public transport would seemingly help to limit PM emissions at all particle sizes.

We strongly recommend extending high-resolution spatiotemporal analyzes of particle distributions per measured $D_P$ bin in urban environments in the future. These analyzes provide a deeper insight into the variability of PNC and particle concentrations than the commonly observed fractions of $PM_1$, $PM_{2.5}$, or $PM_{10}$. They reveal patterns from different emission processes to indicate emission sources which facilitates more effective urban transport planning and eventually a reduction of fine particulate pollution for urban citizens.

## CRediT authorship contribution statement

**Lorenz Harr:** Conceptualization, Methodology, Investigation, Data curation, Visualization, Writing – original draft, Writing – review & editing. **Tim Sinsel:** Data curation, Software, Writing – review & editing. **Helge Simon:** Conceptualization, Writing – review & editing. **Max Carl Arne Torbenson:** Conceptualization, Writing – review & editing. **Esper Jan:** Conceptualization, Supervision, Writing – review & editing.

## Declaration of competing interest

The authors declare that they have no known competing financial interests or personal relationships that could have appeared to influence the work reported in this paper.

## Data availability

Data will be made available on request.

## Acknowledgements

## Appendix A. Supplementary data

Supplementary data to this article can be found online at https://doi.org/10.1016/j.atmosenv.2023.120164.

## References

Azarmi, F., Kumar, P., Marsh, D., Fuller, G., 2016. Assessment of the long-term impacts of PM10 and PM2.5 particles from construction works on surrounding areas. Environmental science. Processes & impacts 18 (2), 208–221. https://doi.org/10.1039/c5em00549c.

Berghmans, P., Bleux, N., Panis, L.I., Mishra, V.K., Torfs, R., Van Poppel, M., 2009. Exposure assessment of a cyclist to PM10 and ultrafine particles. Sci. Total Environ. 407, 1286–1298. https://doi.org/10.1016/j.scitotenv.2008.10.041.

Bonett, D.G., 2006. Confidence interval for a coefficient of quartile variation. Comput. Stat. Data Anal. 50 (11), 2953–2957. https://doi.org/10.1016/j.csda.2005.05.007.

Boogaard, H., Borgman, F., Kamminga, J., Hoek, G., 2009. Exposure to ultrafine and fine particles and noise during cycling and driving in 11 Dutch cities. Atmos. Environ. 43, 4234–4242. https://doi.org/10.1016/j.atmosenv.2009.05.035.

Bukowiecki, N., Lienemann, P., Hill, M., Furger, M., Richard, A., Amato, F., Prévôt, A., Baltensperger, U., Buchmann, B., Gehrig, R., 2010. PM10 emission factors for non-exhaust particles generated by road traffic in an urban street canyon and along a freeway in Switzerland. Atmos. Environ. 44 (19), 2330–2340. https://doi.org/10.1016/j.atmosenv.2010.03.039.

Carreras, H., Ehrnsperger, L., Klemm, O., Paas, B., 2020. Cyclists' exposure to air pollution: in situ evaluation with a cargo bike platform. Environ. Monit. Assess. 192 (7), 470. https://doi.org/10.1007/s10661-020-08443-7.

Ding, N., Prasad, K., Lie, T.T., 2017. The electric vehicle: a review. Int. J. Electr. Hybrid Veh. (IJEHV) 9, 49. https://doi.org/10.1504/IJEHV.2017.082816.

DWD, 2021a. Niederschlag: Vieljährige Mittelwerte 1981 - 2010. DWD. https://www.dwd.de/DE/leistungen/klimadatendeutschland/mittelwerte/nieder_8110_fest.html.html?view=nasPublication&nn=16102. (Accessed 31 August 2022).

DWD, 2021b. Temperatur: Vieljährige Mittelwerte 1981 - 2010. DWD. https://www.dwd.de/DE/leistungen/klimadatendeutschland/mittelwerte/temp_8110_fest.html.html%3Fview%3DnasPublication. (Accessed 31 August 2022).

DWD, 2022. Extracted from Climate Data Center (CDC): monthly station observations of precipitation in mm for Germany. Lerchenberg v21.3. (Accessed 2 September 2022).

Elen, B., Peters, J., Poppel, M., Bleux, N., Theunis, J., Reggente, M., Standaert, A., 2012. The Aeroflex: a bicycle for mobile air quality measurements. Sensors 13, 221–240. https://doi.org/10.3390/s130100221.

European Parliament and Council (EU), 2008. Directive 2008/50/EC of the European Parliament and of the Council of 21 May 2008 on Ambient Air Quality and Cleaner Air for Europe. https://eur-lex.europa.eu/eli/dir/2008/50/oj.

Fussell, J.C., Franklin, M., Green, D.C., Gustafsson, M., Harrison, R.M., Hicks, W., Kelly, F.J., Kishta, F., Miller, M.R., Mudway, I.S., Oroumiyeh, F., Selley, L., Wang, M., Zhu, Y., 2022. A review of road traffic-derived non-exhaust particles: emissions, physicochemical characteristics, health risks, and mitigation measures.

Environ. Sci. Technol. 56 (11), 6813–6835. https://doi.org/10.1021/acs.est.2c01072.

Gallagher, J., Baldauf, R., Fuller, C.H., Kumar, P., Gill, L.W., McNabola, A., 2015. Passive methods for improving air quality in the built environment: a review of porous and solid barriers. Atmos. Environ. 120, 61–70. https://doi.org/10.1016/j.atmosenv.2015.08.075.

Garcia-Algar, O., Canchucaja, L., d'Orazzio, V., Manich, A., Joya, X., Vall, O., 2015. Different exposure of infants and adults to ultrafine particles in the urban area of Barcelona. Environ. Monit. Assess. 187 (1), 4196. https://doi.org/10.1007/s10661-014-4196-5.

GRIMM Aerosol Technik GmbH & Co. KG, 2015. Portable Laser Aerosol Spectrometer: Model Mini-LAS 11-R.

Gualtieri, M., Ovrevik, J., Mollerup, S., Asare, N., Longhin, E., Dahlman, H.-J., Camatini, M., Holme, J.A., 2011. Airborne urban particles (Milan winter-PM2.5) cause mitotic arrest and cell death: effects on DNA, mitochondria, AhR binding and spindle organization. Mutat. Res. 713 (1–2), 18–31. https://doi.org/10.1016/j.mrfmmm.2011.05.011.

Harr, L., Sinsel, T., Simon, H., Esper, J., 2022a. Seasonal changes in urban PM2.5 hotspots and sources from low-cost sensors. Atmosphere 13 (5), 694. https://doi.org/10.3390/atmos13050694.

Harr, L., Sinsel, T., Simon, H., Konter, O., Dreiseitl, D., Schulz, P., Esper, J., 2022b. PM2.5 exposure differences between children and adults. Urban Clim. 44, 101198 https://doi.org/10.1016/j.uclim.2022.101198.

Harrison, R.M., Allan, J., Carruthers, D., Heal, M.R., Lewis, A.C., Marner, B., Murrells, T., Williams, A., 2021. Non-exhaust vehicle emissions of particulate matter and VOC from road traffic: a review. Atmos. Environ. 262, 118592 https://doi.org/10.1016/j.atmosenv.2021.118592.

Hussein, T., Johansson, C., Karlsson, H., Hansson, H.-C., 2008. Factors affecting non-tailpipe aerosol particle emissions from paved roads: on-road measurements in Stockholm, Sweden. Atmos. Environ. 42 (4), 688–702. https://doi.org/10.1016/j.atmosenv.2007.09.064.

Jalava, P.I., Wang, Q., Kuuspalo, K., Ruusunen, J., Hao, L., Fang, D., Väisänen, O., Ruuskanen, A., Sippula, O., Happo, M.S., Uski, O., Kasurinen, S., Torvela, T., Koponen, H., Lehtinen, K., Komppula, M., Gu, C., Jokiniemi, J., Hirvonen, M.-R., 2015. Day and night variation in chemical composition and toxicological responses of size segregated urban air PM samples in a high air pollution situation. Atmos. Environ. 120, 427–437. https://doi.org/10.1016/j.atmosenv.2015.08.089.

Karagulian, F., Belis, C.A., Dora, C.F.C., Prüss-Ustün, A.M., Bonjour, S., Adair-Rohani, H., Amann, M., 2015. Contributions to cities' ambient particulate matter (PM): a systematic review of local source contributions at global level. Atmos. Environ. 120, 475–483. https://doi.org/10.1016/j.atmosenv.2015.08.087.

Klemm, O., Ahrens, A., Arnswald, M., Bethke, R., Berger, D.F., Blankenhaus, K., Blauth, L., Breuer, B., Buchholz, S., Burek, F., Ehrnsperger, L., Funken, S., Henninger, E., Hohl, J., Jöllenbeck, N., Kirgasser, P., Kuhls, M., Paas, B., Roters, L.A., Schaller, C., Schlüter, H., 2021. The impact of traffic and meteorology on urban particle mass and particle number concentrations: student-led studies using mobile measurements before, during, and after the COVID-19 pandemic lockdowns. Atmosphere 13, 62. https://doi.org/10.3390/atmos13010062.

Kerschbaumer, A., Lutz, M., 2008. Origin and influence of PM10 in urban and in rural environments. Adv. Sci. Res. 2 (1), 53–55. https://doi.org/10.5194/asr-2-53-2008.

Lelieveld, J., Klingmüller, K., Pozzer, A., Pöschl, U., Fnais, M., Daiber, A., Münzel, T., 2019. Cardiovascular disease burden from ambient air pollution in Europe reassessed using novel hazard ratio functions. Eur. Heart J. 40 (20), 1590–1596. https://doi.org/10.1093/eurheartj/ehz135.

Lough, G.C., Schauer, J.J., Park, J.-S., Shafer, M.M., Deminter, J.T., Weinstein, J.P., 2005. Emissions of metals associated with motor vehicle roadways. Environ. Sci. Technol. 39 (3), 826–836. https://doi.org/10.1021/es048715f.

Mie, G., 1908. Beiträge zur Optik trüber Medien, speziell kolloidaler Metallösungen. Ann. Phys. 330 (3), 377–445. https://doi.org/10.1002/ANDP.19083300302.

Minguillón, M.C., Querol, X., Baltensperger, U., Prévôt, A.S.H., 2012. Fine and coarse PM composition and sources in rural and urban sites in Switzerland: local or regional pollution? Sci. Total Environ. 427–428, 191–202. https://doi.org/10.1016/j.scitotenv.2012.04.030.

Morawska, L., Johnson, G., Ristovski, Z.D., Agranovski, V., 1999. Relation between particle mass and number for submicrometer airborne particles. Atmos. Environ. 33 (13), 1983–1990. https://doi.org/10.1016/S1352-2310(98)00433-6.

Oroumiyeh, F., Zhu, Y., 2021. Brake and tire particles measured from on-road vehicles: effects of vehicle mass and braking intensity. Atmos. Environ. X 12, 100121. https://doi.org/10.1016/j.aeaoa.2021.100121.

Peters, T.M., Ott, D., O'Shaughnessy, P.T., 2006. Comparison of the Grimm 1.108 and 1.109 portable aerosol spectrometer to the TSI 3321 aerodynamic particle sizer for dry particles. Ann. Occup. Hyg. 50 (8), 843–850. https://doi.org/10.1093/annhyg/mel067.

Piscitello, A., Bianco, C., Casasso, A., Sethi, R., 2021. Non-exhaust traffic emissions: sources, characterization, and mitigation measures. Sci. Total Environ. 766, 144440 https://doi.org/10.1016/j.scitotenv.2020.144440.

Sanders, P.G., Xu, N., Dalka, T.M., Maricq, M.M., 2003. Airborne brake wear debris: size distributions, composition, and a comparison of dynamometer and vehicle tests. Environ. Sci. Technol. 37 (18), 4060–4069. https://doi.org/10.1021/es034145s.

Sanguesa, J.A., Torres-Sanz, V., Garrido, P., Martinez, F.J., Marquez-Barja, J.M., 2021. A review on electric vehicles: technologies and challenges. Smart Cities 4, 372–404. https://doi.org/10.3390/smartcities4010022.

Samad, A., Vogt, U., 2020. Investigation of urban air quality by performing mobile measurements using a bicycle (MOBAIR). Urban Clim. 33, 100650 https://doi.org/10.1016/j.uclim.2020.100650.

Schraufnagel, D.E., 2020. The health effects of ultrafine particles. Exp. Mol. Med. 52 (3), 311–317. https://doi.org/10.1038/s12276-020-0403-3.

Sharma, A., Kumar, P., 2020. Quantification of air pollution exposure to in-pram babies and mitigation strategies. Environ. Int. 139, 105671 https://doi.org/10.1016/j.envint.2020.105671.

Shepard, D., 1968. A two-dimensional interpolation function for irregularly-spaced data. In: Proceedings of the 1968 23rd ACM National Conference on -. The 1968 23rd ACM National Conference, Not Known. ACM Press, New York, New York, USA, pp. 517–524. https://doi.org/10.1145/800186.810616.

Squizzato, S., Masiol, M., Agostini, C., Visin, F., Formenton, G., Harrison, R.M., Rampazzo, G., 2016. Factors, origin and sources affecting PM 1 concentrations and composition at an urban background site. Atmos. Res. 180, 262–273. https://doi.org/10.1016/j.atmosres.2016.06.002.

Stewart, I.D., Oke, T.R., 2012. Local climate zones for urban temperature studies. Bull. Am. Meteorol. Soc. 93 (12), 1879–1900. https://doi.org/10.1175/BAMS-D-11-00019.1.

Tang, G., Zhang, J., Zhu, X., Song, T., Münkel, C., Hu, B., Schäfer, K., Liu, Z., Zhang, J., Wang, L., Xin, J., Suppan, P., Wang, Y., 2016. Mixing layer height and its implications for air pollution over Beijing, China. Atmos. Chem. Phys. 16 (4), 2459–2475. https://doi.org/10.5194/acp-16-2459-2016.

Timmers, V.R.J.H., Achten, P.A.J., 2016. Non-exhaust PM emissions from electric vehicles. Atmos. Environ. 134, 10–17. https://doi.org/10.1016/j.atmosenv.2016.03.017.

Titos, G., Lyamani, H., Pandolfi, M., Alastuey, A., Alados-Arboledas, L., 2014. Identification of fine (PM1) and coarse (PM10-1) sources of particulate matter in an urban environment. Atmos. Environ. 89, 593–602. https://doi.org/10.1016/j.atmosenv.2014.03.001.

Torres-Ramos, Y.D., Montoya-Estrada, A., Guzman-Grenfell, A.M., Mancilla-Ramirez, J., Cardenas-Gonzalez, B., Blanco-Jimenez, S., Sepulveda-Sanchez, J.D., Ramirez-Venegas, A., Hicks, J.J., 2011. Urban PM2.5 induces ROS generation and RBC damage in COPD patients. Frontiers in bioscience (Elite edition) 3, 808–817. https://doi.org/10.2741/e288.

Van den Bossche, J., Peters, J., Verwaeren, J., Botteldooren, D., Theunis, J., De Baets, B., 2015. Mobile monitoring for mapping spatial variation in urban air quality: development and validation of a methodology based on an extensive dataset. Atmos. Environ. 105, 148–161. https://doi.org/10.1016/j.atmosenv.2015.01.017.

Wagner, P., Schäfer, K., 2017. Influence of mixing layer height on air pollutant concentrations in an urban street canyon. Urban Clim. 22, 64–79. https://doi.org/10.1016/j.uclim.2015.11.001.

Who, 2022. World Health Statistics 2022: Monitoring Health for the SDGs, Sustainable Development Goals. Global Report. World Health Organization (WHO).

Woo, S.-H., Jang, H., Lee, S.-B., Lee, S., 2022. Comparison of total PM emissions emitted from electric and internal combustion engine vehicles: an experimental analysis. Sci. Total Environ. 842, 156961 https://doi.org/10.1016/j.scitotenv.2022.156961.

Wu, Y., Liu, J., Zhai, J., Cong, L., Wang, Y., Ma, W., Zhang, Z., Li, C., 2018. Comparison of dry and wet deposition of particulate matter in near-surface waters during summer. PLoS One 13 (6), e0199241. https://doi.org/10.1371/journal.pone.0199241.

Yang, M., Guo, Y.-M., Bloom, M.S., Dharmagee, S.C., Morawska, L., Heinrich, J., Jalaludin, B., Markevychd, I., Knibbsf, L.D., Lin, S., Hung Lan, S., Jalava, P., Komppula, M., Roponen, M., Hirvonen, M.-R., Guan, Q.-H., Liang, Z.-M., Yu, H.-Y., Hu, L.-W., Yang, B.-Y., Zeng, X.-W., Dong, G.-H., 2020. Is PM1 similar to PM2.5? A new insight into the association of PM1 and PM2.5 with children's lung function. Environ. Int. 145, 106092 https://doi.org/10.1016/j.envint.2020.106092.

Yong, J.Y., Ramachandaramurthy, V.K., Tan, K.M., Mithulananthan, N., 2015. A review on the state-of-the-art technologies of electric vehicle, its impacts and prospects. Renew. Sustain. Energy Rev. 49, 365–385. https://doi.org/10.1016/j.rser.2015.04.130.

ZIMEN, 2021. Jahresbericht 2020: Zentrales Immissionsmessnetz - ZIMEN -. ZIMEN. https://luft.rlp.de/fileadmin/luft/ZIMEN/Jahresberichte/ZIMEN-Jahresbericht_2020.pdf. (Accessed 31 August 2022).

ZIMEN, 2022. Luft-überwachung in rheinland-pfalz -: zentrales immissionsmessnetz - ZIMEN -. State office of rhineland-palatinate. https://luft.rlp.de/de/startseite/.